JOURNAL OF MATERIALS SCIENCE 20 (1985) 3184 - 3190

Fractography of the interlaminar fracture of carbon-fibre epoxy composites

W. D. BASCOM, D. J. BOLL
Hercules Aerospace, Hercules, Inc, Magna, Utah, USA

B. FULLER*, P. J. PHILLIPS
Department of Materials Science and Engineering, University of Utah, Salt Lake City, Utah, USA

The failed surfaces of interlaminar fracture (mode I) specimens of AS4/3501-6 were examined using scanning electron microscopy. The principle fracture features were fibre pull-out (bundles and single fibres), hackle markings and regions of smooth resin fracture. Considerable (30 to 50%) relaxation of the deformed resin occurred when the specimens were heated above the matrix T_g. This relaxation was taken as evidence of extensive shear yielding of the resin during the fracture process. Some of the fractography features are discussed in terms of transverse tensile stresses and peeling stresses acting on the fibres. In some instances these localized stresses focus failure close to the resin–fibre interface which can be mistakenly interpreted as interfacial failure and low fibre–resin adhesion.

1. Introduction

The interlaminar fracture of continuous carbon-fibre reinforced compsites has been the subject of numerous investigations [1–5]. The majority of this work has been done using double cantilever beam specimens which, from a continuum point of view, measures an opening mode (mode I) interlaminar fracture energy, $\mathcal{G}_{IC}$. However, the microdeformation processes in the crack tip damage zone are undoubtedly more complex and involve combined shear and tensile components. Sinclair and Chamis [6], Morris [7], Miller and Wingert [8], Johannesson *et al.* [9], and Richards-Frandsen and Naerheim [10] have reported hackle (serrations or tear) marking as well as loose and broken fibre some of which appears to have pulled away from the matrix at the fibre–resin interface. Russell and Street [11] have presented photomicrographs of delamination under mixed-mode loadings which show hackle markings but no clear correlation between hackle configuration and the load ratio, mode I/mode II. Bradley and Cohen [5] observed the development of the damage zone in a scanning electron microscope (SEM) and noted matrix cracking and apparent interfacial fibre failure. They observed a much larger region of damage above and below the main crack front for composites with "ductile" matrix resins than for "brittle" matrix resins. Many authors have noted fibre bridging across the crack opening sufficient to create a "tied zone" [11]. de Charentenay and Benzeggagh [12] detected damage well ahead of the apparent crack front using acoustic emission techniques.

In the work reported here, preliminary results are presented on the fractographic features associated with interlaminar fracture. Interpretation of these features gives some insight as to the deformation processes in the crack front damage zone. Double cantilever beam specimens of Hercules AS-4/3501-6 that had been tested for interlaminar $\mathcal{G}_{IC}$ [13] were examined using high resolution SEM. In order to determine if any of the features were the result of plastic deformation, the specimens were heated

*Present address: IBM, Endicott, New York, USA.

0022–2461/85 $03.00 + .12

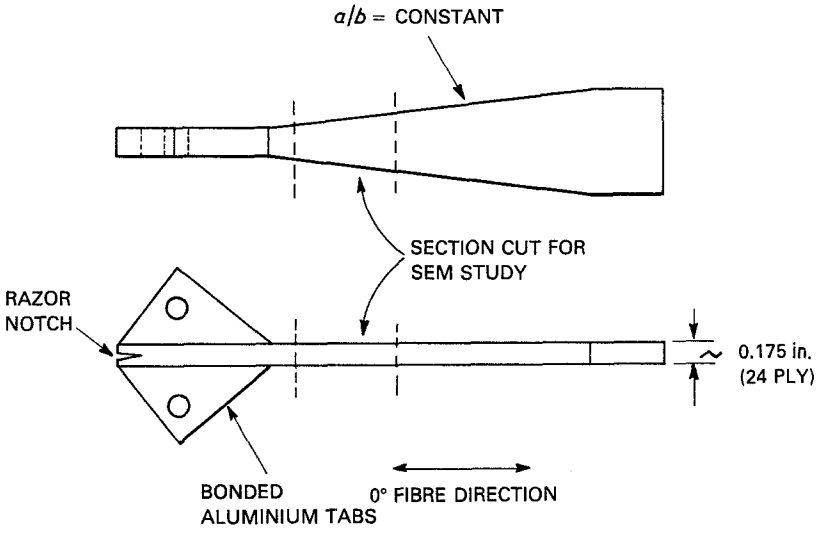

Figure 1 Schematic illustration of width tapered double cantilever beam specimen showing section cut for SEM examination.

above the resin T_g and then examined for changes in appearance.

2. Experimental details

Width tapered double cantilever beam (WTDCB) specimens were fabricated from AS4/3501-6 prepreg by hand lay-up of 24 ply (~ 3 mm) unidirectional panels and autoclave cured at 350° F (177° C) for 2 h and post-cured at 350° F for 4 h. The WTDCB specimens were cut from the cured panels with the 0° fibre direction along the length of the specimen in all cases. These specimens had been tested for interlaminar $\mathcal{G}_{IC}$ [13] and gave an average value of $190 \pm 10\,J\,m^{-2}$ ($1.09\,in.lb\,in^{-2}$). Sections were cut from the tapered region as shown in Fig 1. The fracture load (and thus the fracture energy) was essentially constant through the tapered section. Specimens measuring 4 mm × 6 mm in cross-section and 1.5 mm thick (12 plys) were cut and mounted for SEM examination. A thin (10 to 20 nm) gold coating was deposited to reduce charging. The SEM was a JOEL 200Cx scanning transmission electron microscope used in the normal electron scanning mode. Because of the relatively large specimen size the tilt angle was fixed at 90°. In those instances where it was necessary to vary the tilt angle, a Cambridge Stereoscan II was used with some loss in resolution compared to the JOEL microscope.

3. Results

Three major features that characterize much of the fracture surfaces are shown in Fig. 2, being fibre pull-out, matrix fracture and hackle markings. Fibre pull-out and break-off are shown in Figs. 2a and b. The right-hand side of Fig. 2c illustrates a region of smooth resin fracture and Fig. 2d illustrates the hackle marking associated with the pull-out of two adjacent fibres. In general, pull-out involved fibre bundles; in Fig. 2b at least 5 and possibly 8 fibres were drawn from two adjacent layers. The hackle markings in Figs. 2c and b appear to emanate from the periphery of the fibres and form "river marking" at a slight angle toward the direction of crack propagation. (The arrows on the figures indicate the direction of crack propagation.) Note that the troughs left by the fibre between the rows of hackle markings are essentially featureless which suggests relatively little resin deformation.

Fig. 3 also shows fibre pull-out, hackle markings and areas of smooth resin fracture. In addition, a single fibre is shown that extends out of the general plane of fracture at one end but is embedded in the resin at the other. A relatively high magnification view of the loose end (Fig. 3b) suggests that there are "flanges" of resin extending from both sides of the fibre. Fig. 3c illustrates the deformation associated with fibre (or fibre bundle) break-off. In Fig. 3d a flange of resin has developed on one side of the fibre but on the other side was in the process of developing below the plane of fracture.

The effect of thermal relaxation on the

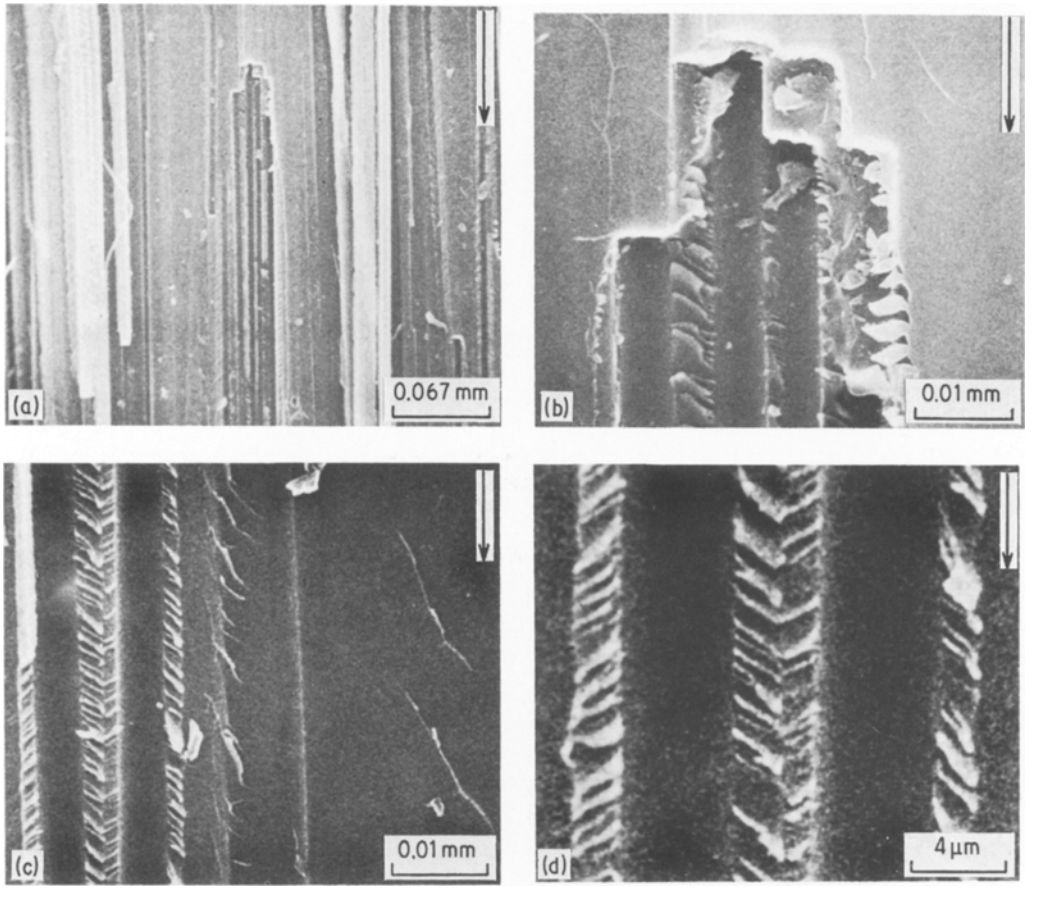

Figure 2 Scanning electron micrograph showing major fractographic features: fibre pull-out, hackle markings, smooth resin fracture.

deformation features is shown in Figs. 4 and 5. Specific locations on the fracture surface were selected and their co-ordinate positions on the microscope stage recorded. The specimen was then removed from the microscope, held at 50° C above resin T_g (225° C) for 10 min, cooled, and repositioned in the microscope and examined for changes in the deformation features.

A comparison of Figs. 4a and b indicates considerable reduction in the size and shape of the deformation after thermal treatment. Notably, a reduction in the size and number of hackle markings, and the width of the flange structure on the fibre in Figs. 4c and d. Some features were unaffected by heating, e.g. the pebble-like fragment in the upper right-hand corner of c and d.

In Fig. 5, a channel left by a pulled-out fibre appears to have been "straightened out" by the thermal treatment. As in Fig. 4, there was a distinct reduction in the number and size of the hackle markings.

A comparison of specific features before and after thermal treatment suggests dimensional reductions of from 30 to 50% and even greater after 10 min at 50° C above T_g. Since the photographs presented in Figs. 4 and 5 were all taken with the beam directed perpendicular to the specimen, some of the apparent dimensional changes could be due to movement of the feature rather than shrinkage. However, examination of these specimens at a tilt angle of 55° established that size changes of 30 to 50% had, in fact, occurred.

Heat treatment at temperatures below T_g, but 10° C above the tenperature at which the elastic modulus of 3501-6 begins to fall abruptly from the glassy to rubbery state, ($T\Delta G'$) produced less dramatic relaxation effects than shown in Figs. 4 and 5. Nonetheless, dimensional changes

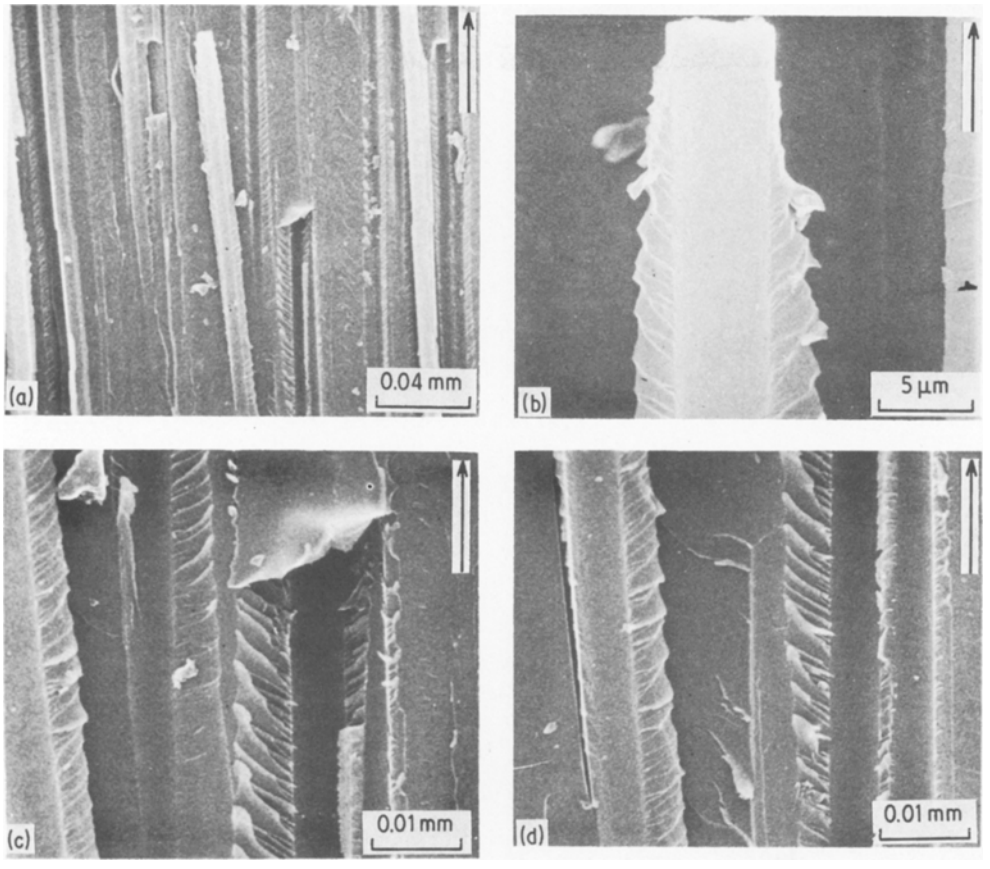

Figure 3 Scanning electron mirograph showing fibre pull-out and flanges of resin extending from the sides of the fibre.

did occur after 10 min at 10° above $T\Delta G'$ for the more severely deformed regions, e.g. the tear features on the right-hand side of Fig. 2b.

4. Discussion

Deformations of even 30% seem rather large for an epoxy such as 3501-6. This polymer is a highly crosslinked thermoset based on the tetraglycidylether of methylene dianiline and diaminodiphenylsulphone with minor amounts of epoxy modifiers and catalysts. In conventional tensile tests (ASTM D 638-60) the elongation is of the order of 2 to 3% or less. On the other hand, studies of epoxy resin fracture [14–16] indicate extensive crack tip yielding of the resin in the initial "slow crack growth" region but that within a short distance this yielding becomes unstable, the crack speed accelerates, and the fracture surface is essentially featureless.

Actually, the conventional tensile testing of matrix resins may be misleading in that a relatively large cross-sectional area (gauge section) is tested compared to the amount of resin between fibres in a laminate (or the initial plastic zone in resin fracture testing). Recently, Odom and Adams [17] found that at cross-sections of less than 0.1 cm^2, there is an exponential increase in resin tensile strength for 3501-6. At conventional dimensions (0.4 cm^2) the tensile strength is $\sim$ 42 MPa but increased to more than 90 MPa at 0.01 cm^2. We might expect even higher strengths (and strains) for dimensions comparable to interfibre distances, 10^{-6} cm^2.

Most of the fractography features can be understood if delamination is considered in a simplistic fashion as a two-step process. Ahead of the main crack front the fibre can be viewed as a high modulus inclusion in a lower modulus matrix subject to essentially tensile stresses normal to the plane of the specimen and the fibre longitudinal axis. In Fig. 6, the stress distribution at the fibre–resin interface is shown for the circumference of an isolated fibre [18, 19]. It predicts that failure will be focused near the

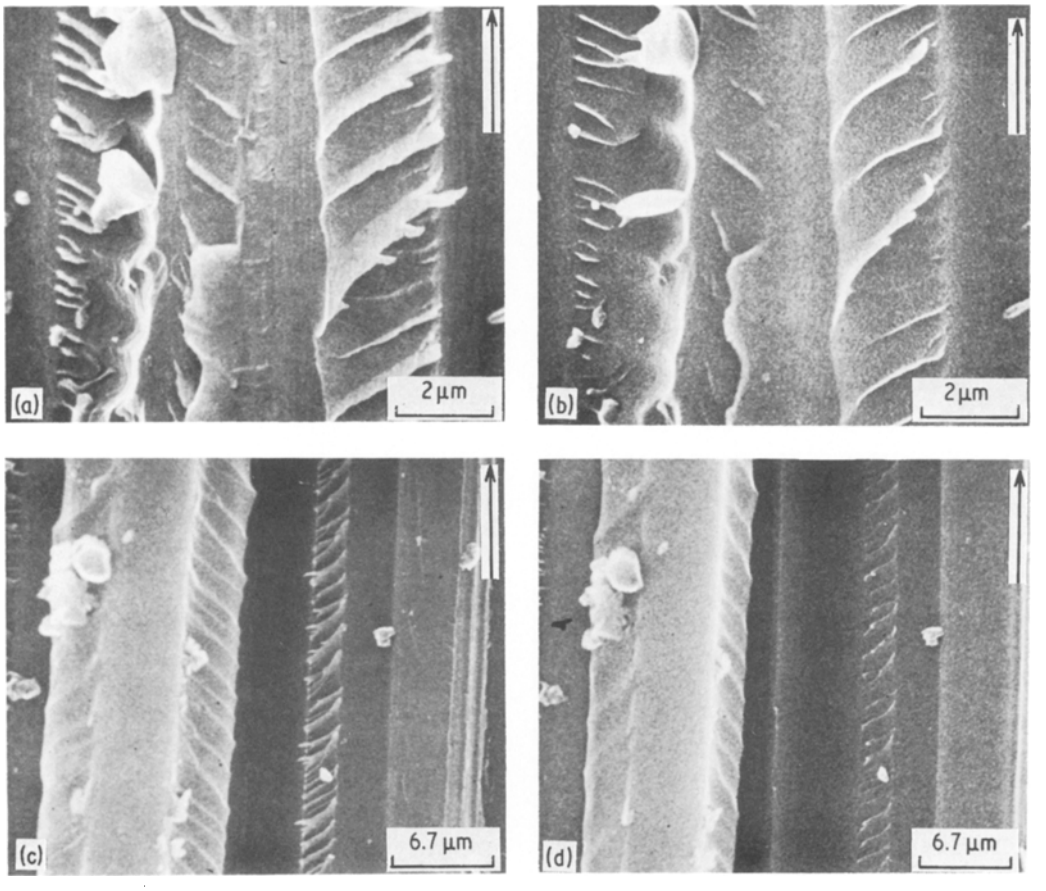

Figure 4 Effects of heating at T_g + 50° C on fractographic features.

fibre–resin interface at the top (and bottom) of the fibre. A resultant shear stress will exist where the radial stress changes from tension to compression and that at this point (a in Fig. 6) there is localized shear yielding of the matrix.

Subsequently, the fibre is "peeled-out" of the resin in the manner shown in Fig. 7. Failure occurs along the boundary (as in Fig. 6) and, for an isolated fibre, would lead to a flange or "wing" of resin on both sides of the fibre; a configuration similar to that shown in Fig. 3b.

The stress distribution known to exist at the

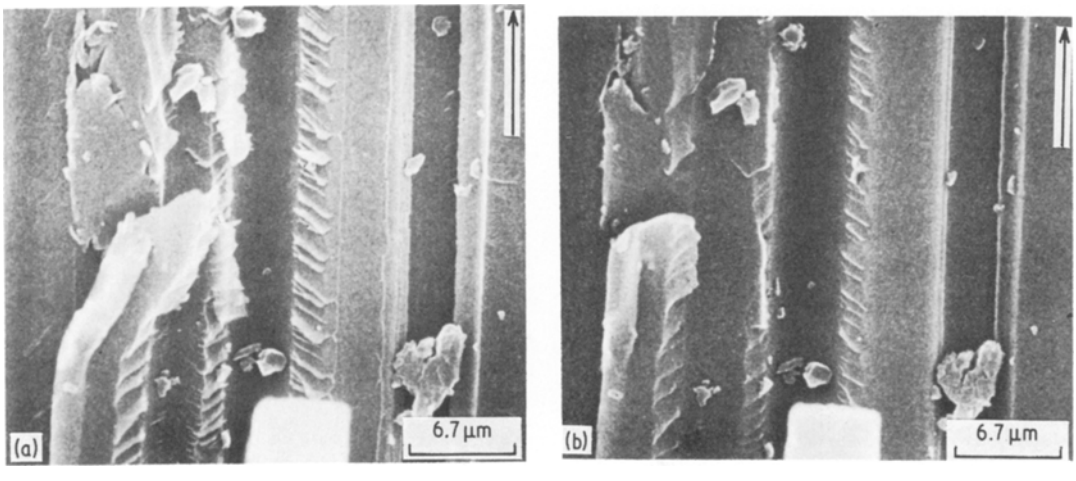

Figure 5 Effects of heating of T_g + 50° C on fractographic features.

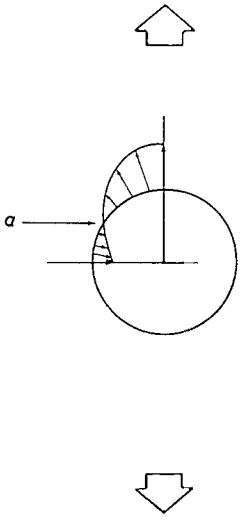

Figure 6 Stress distribution (one quadrant) at the resin/fibre boundary for a fibre in transverse loading.

peel front [20] is also shown in Fig. 7. The combination of tensile and compressive forces tends to focus failure into the interfacial region and thereby add to the apparent interfacial failure at the top and bottom of the fibre.

Resin yielding along the fibre (under tensile loading. Fig. 6 or peel-out, Fig. 7) is not uniform but appears to be nucleated from closely spaced sites in the material or stress inhomogeneities along the fibre–resin boundry. Discrete yielding sites are also observed in the slow growth yield zone of cracks in resin [14]. Ligaments form across the crack opening which rupture to leave fracture markings not unlike the hackle markings observed here.

The hackle markings, especially near isolated fibres, are bounded by areas of featureless resin fracture which presumably correspond to slow growth failure becoming unstable and the onset of catastrophic fast fracture.

The high level of shear yielding, revealed by relaxation of the fractographic features when heated above T_g, results from the localized nature of the yielding processes. If this yielding leads to the formation of ligaments, the latter will deform under plane stress conditions so that there is little lateral constraint to inhibit elongation. Intersection of the yield zones of adjacent fibres may have a reinforcing effect which also augments elongation.

Unquestionably, the overall deformation processes in mode I delamination are more complex than depicted here. A more detailed analysis would be necessary to understand fibre bundle pull-out, fibre fracture, fibre cross-over effects and crack front branching.

Previous post failure studies of interlaminar fracture have all reported hackle markings as a predominate fractography feature. These markings have been referred to as hackle, serrations, lacerations and chevrons. Morris [7] was able to relate the hackle tilt directions to the direction of crack propagation, Richards-Frandsen and Naerheim [10] related the spacing of the hackle markings to interfibre spacing, and Russell and Street [11] showed the effect of combined loading (pure and mixed modes I and II) on hackle appearance and spacing. There was no attempt in any of these studies to determine if the hackles result from brittle or ductile resin deformation. Sinclair and Chamis [6] refer to hackle formation as a resin tearing which implies yielding, whereas Morris [7] proposes a mechanism for hackle formation by brittle resin cracking.

Comparisons of earlier work with the present study are complicated by differences in the

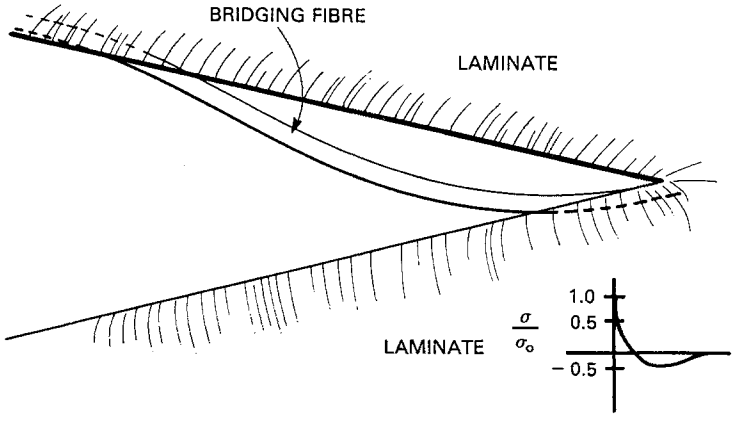

Figure 7 Peel-out of fibres at the delamination showing the distribution of tensile and compressive stresses.

methods used to create delamination. Previous studies involved mixed-mode loadings with large shear components, whereas the WTDCB specimens used here involved primarily tensile loads. The results presented by Russell and Street [11] give some indication of how increasing mode II affects hackle marking but a more detailed investigation is needed.

5. Conclusions

The principle fractography features observed on the failed surfaces of carbon-fibre composites after mode I delamination include loose fibre, channels formed by fibre pull-out, hackle markings, and regions of smooth resin fracture. Heating the specimen to 50° C above the resin T_g caused extensive relaxation of much of the resin deformation. This relaxation suggests that the resin had undergone extensive (30 to 50% and higher) shear yielding during the fracture process. An idealized consideration of the stresses on a single, isolated fibre in the fracture plane suggests that yielding occurs along the fibre–resin boundary near the fibre midplane. Subsequently, the fibre is pulled (peeled) out of the resin matrix and fractures. The transverse stresses and peeling stresses tend to focus failure close to the fibre/resin interface near the top and bottom of the fibre but tearing and possibly ligament formation in the fibre plane are believed responsible for the extensive hackle markings. Mechanical focusing of failure close to the fibre–resin boundary can be erroneously interpreted as interfacial failure and low fibre–resin adhesion. This same phenomenon has been studied in the case of mixed-mode adhesive bond fracture [21, 22].

Acknowledgements

The authors wish to express their appreciation to Dr Brian Swetlin (Hercules, Inc, Research Center) for very helpful suggestions. Part of this work was supported by NASA with much encouragement from Dr Norman J. Johnston (NASA, Langley Research Center).

References

1. G. B. McKENNA, *Polymer-Plast. Technol. Eng.* **5** (1975) 23.
2. D. F. DEVITT, R. A. SCHAPERY and W. L. BRADLEY, *Compos. Mater.* **14** (1980) 271.
3. J. M. WHITNEY, C. E. BROWNING and W. J. HOAGSTEDEN, *Reinforced Plastics and Composites* **1** (1982) 297.
4. W. D. BASCOM, J. L. BITNER, R. J. MOULTON and A. R. SIEBERT, *Composites* **11** (1980) 9.
5. W. L. BRADLEY and R. N. COHEN, ASTM Symposium on Delamination and Debonding of Materials, Pittsburg, Pennsylvania, November (1983).
6. J. H. SINCLAIR and C. C. CHAMIS, "Mechanical Behavior and Fracture Characteristics of Off Axis Fiber Composites I Experimental Investigation", NASA Technical Paper 1081, NASA, Washington DC, December (1977).
7. G. E. MORRIS, "Nondestructive Evaluation and Flaw Criticality for Composite Materials", ASTM STP 696, edited by R. B. Pipes (American Society for Testing and Materials, Philadelphia, Pennsylvania, 1979) p. 274.
8. A. G. MILLER and A. L. WINGERT, *ibid.*, p. 223.
9. T. JOHANNESSON, P. SJOBLOM and R. SELDEN, *J. Mater. Sci.* **19** (1984) 1171.
10. R. RICHARDS-FRANDSEN and Y. NAERHEIM, *J. Compos. Mater.* **17** (1983) 105.
11. A. J. RUSSELL and K. N. STREET, Proceedings 4th International Conference on Composite Materials, 1982 ICCM-IV, Tokyo, p. 279.
12. F. X. de CHARENTENAY and M. BENZEGAGH, "Advances in Composite Materials, Proceedings" ICCM-3, Vol. 1 (Pergamon Press, Oxford, 1980) p. 186.
13. W. D. BASCOM, G. W. BULLMAN, D. L. HUNSTON and R. M. JENSEN, 29th National SAMPE Symposium, Reno Proceedings, Vol. 29 (1984) p. 970.
14. R. L. PATRICK, in "Treatise on Adhesion and Adhesives", edited by R. L. Patrick, (1973) Ch.4, p. 163.
15. W. D. BASCOM, R. L. COTTINGTON, R. L. JONES and P. PEYSER, *J. Appl. Polym. Sci.* **19** (1975) 2545.
16. W. D. BASCOM, R. Y. TING, R. J. MOULTON, C. V. RIEW and A. R. SIEBERT, *J. Mater. Sci.* **16** (1981) 2657.
17. E. M. ODOM and D. F. ADAMS, College of Engineering, University of Wyoming, private communication (1983).
18. H. SCHUIECH, "Mechanics of Composite Materials", edited by F. W. Wendt, H. Liebowitz, N. Perrone, Proceedings of the 5th Symposium on Naval Structural Mechanics, Philadelphia (Pergamon Press, New York, 1967).
19. G. H. NEWAG, *SAMPE Quart.* **15** (1984) 20.
20. D. H. KAELBLE, in "Adhesion and Cohesion", edited by P. Weiss (Elsevier, New York, 1962) p. 74.
21. W. D. BASCOM, C. O. TIMMONS and R. L. JONES, *J. Mater. Sci.* **10** (1975) 1037.
22. W. D. BASCOM and J. OROSHNIK, *ibid.* **13** (1978) 1411.

Received 24 September
and accepted 15 October 1984